Cell-specific deletion of glucosylceramide synthase in brain leads to severe neural defects after birth

Richard Jennemann*†, Roger Sandhoff*, Shijun Wang*, Eva Kiss*, Norbert Gretz‡, Cecilia Zuliani§, Ana Martin-Villalba§, Richard Jäger¶, Hubert Schorle¶, Marc Kenzelmann*, Mahnaz Bonrouhi*, Herbert Wiegandt*, and Hermann-Josef Gröne*†

Abteilungen *Zelluläre und Molekulare Pathologie and §Immungenetik, Deutsches Krebsforschungszentrum Heidelberg, Im Neuenheimer Feld 280, 69120 Heidelberg, Germany; ‡Zentrum für Medizinische Forschung, Ruprecht-Karls-Universität Heidelberg, Theodor-Kutzer-Ufer, 68167 Mannheim, Germany; and ¶Abteilung Entwicklungspathologie, Institut für Pathologie, Universitätsklinikum Bonn, Sigmund-Freud-Strasse 25, 53127 Bonn, Germany

Edited by Sen-itiroh Hakomori, Pacific Northwest Research Institute, Seattle, WA, and approved July 11, 2005 (received for review February 3, 2005)

Sialic acid-containing glycosphingolipids, i.e., gangliosides, constitute a major component of neuronal cells and are thought to be essential for brain function. UDP-glucose:ceramide glucosyltransferase (Ugcg) catalyzes the initial step of glycosphingolipid (GSL) biosynthesis. To gain insight into the role of GSLs in brain development and function, a cell-specific disruption of Ugcg was performed as indicated by the absence of virtually all glucosylceramide-based GSLs. Shortly after birth, mice showed dysfunction of cerebellum and peripheral nerves, associated with structural defects. Axon branching of Purkinje cells was significantly reduced. In primary cultures of neurons, dendritic complexity was clearly diminished, and pruning occurred early. Myelin sheaths of peripheral nerves were broadened and focally severely disorganized. GSL deficiency also led to a down-regulation of gene expression sets involved in brain development and homeostasis. Mice died ≈3 weeks after birth. These results imply that GSLs are essential for brain maturation.

glycosphingolipid | ceramide | neuron differentiation | myelin

Glycosphingolipids (GSLs)‖ with their lipophilic ceramide linked to a great variety of complex carbohydrate residues are typical amphipathic membrane constituents of eukaryotic cells. A major portion of the GSLs is located on the outer leaflet of the cellular plasma membrane where they may act in the assembly of signaling molecules (2, 3), modulation of cell adhesion (4), and differentiation (5). Intracellularly, GSLs may be important for protein trafficking (6).

All mammalian GSLs are synthesized either on the cytoplasmic surface of the Golgi complex by enzyme-catalyzed addition of UDP-activated glucose to ceramide, or on the luminal side of the endoplasmic reticulum with UDP-galactose (7) (Fig. 1 *A* and *B*). The resulting gluco- or galactocerebrosides may be further substituted by enzyme-catalyzed addition of monosaccharides at the luminal side of the Golgi complex. Acidic GSLs, i.e., sulfatides and gangliosides, are formed by addition of sulfate or neuraminic acid residues, respectively. Whereas only comparatively few GSLs are derived from galactocerebroside, hundreds of structurally different GSLs, including higher sulfatides and gangliosides, are known to contain the glucosylceramide (GlcCer) core, emphasizing the potential physiological importance of this precursor molecule (Fig. 1*A*).

The mouse GlcCer synthase (Ugcg; UDP-glucose:ceramide glucosyltransferase, EC 2.4.1.80) gene was initially cloned by Hirabayashi *et al.* (8). It was shown that disruption of the *Ugcg* gene in mice resulted in embryonic lethality during gastrulation at embryonic day 6.5 (E6.5) to E7.5 (9). To obtain more insight into the organ-specific function of the *Ugcg* gene, a cell-specific functional deletion was performed. Central nervous tissue contains comparably high concentrations of GSLs, specifically gangliosides (10). In view of the assumed importance of GSLs in the brain, mice were generated that carry the nestin gene promoter-driven *cre* transgene (11) in combination with an *Ugcg*-null and "floxed" allele. The resulting neural cell-specific disruption of the formation of glucocerebroside-derived GSLs did not impair late embryonic development. However, all Ugcg-deficient mice died between postnatal day 11 (P11) and P24. Our results indicate that GSLs are required for brain maturation after birth.

Materials and Methods

Construction of the Targeting Vector. An ≈8-kb Sst I/Sal I DNA fragment of the *Ugcg* gene (National Center for Biotechnology Information accession no. NP 035803), containing exon 5 to exon 9 and a part of the 3′ ORF, was cloned into pBluescript (Stratagene). A HSVtk–PGKneo selection cassette, which was flanked by FLP recombination target (FRT) sites and one 5′ single loxP site, was inserted into a Nhe I site between exons 5 and 6 (Fig. 1*C*). A diagnostic Nde I site was introduced at the 5′ end of the HSVtk–PGKneo cassette. A second loxP site and a preceding diagnostic Spe I site were inserted into Eco 47 III between exons 8 and 9 (Fig. 1*C*).

E14 ES cells were transfected in the presence of the linearized *Ugcg*-targeting vector and cultivated as described in ref. 12. For genotyping, see Fig. 1 *D* and *E* and *Supporting Methods*, which is published as supporting information on the PNAS web site.

Generation of Germ-Line Chimeras, as Well as Null and Floxed Mice. Positive ES cells were injected into blastocysts from C57BL/6 mice. Mutant mice were characterized by Southern and PCR analysis of genomic DNA of tail biopsies as described in *Supporting Methods*. *Ugcg*-null and -floxed mice were generated by breeding $Ugcg^{\text{flox-tkneo}}$ mice with *cre*- (13) and FLP-deleter mice (14) (Fig. 1 *F–H*).

Neural cell-specific Ugcg-deficient animals were generated by breeding mice expressing Cre recombinase under control of the nestin gene promoter (11) with heterozygous $Ugcg^{\text{null/+}}$ mice. The resulting $Ugcg^{\text{null/+//NesCre}}$ mice were further mated with $Ugcg^{\text{flox/flox}}$ mice, resulting in $Ugcg^{\text{null/flox//NesCre}}$ mice.

Isolation of GSLs and Electrospray Ionization/Tandem Mass Spectrometry (ESI-MS/MS). GSLs were isolated (15) and prepared for ESI MS/MS quantifications as described in ref. 16. The $Ugcg^{\text{null/flox//NesCre}}$ mice and controls investigated were E15.5 ($n = 2$), P0 ($n = 2$), P5 ($n = 3$), P10 ($n = 5$), and P15 ($n = 5$).

This paper was submitted directly (Track II) to the PNAS office.

Abbreviations: GSL, glycosphingolipid; Ugcg, UDP-glucose:ceramide glucosyltransferase; GlcCer, glucosylceramide; E*n*, embryonic day *n*; P*n*, postnatal day *n*; FRT, FLP recombination target; GalNAcT, *N*-acetylgalactosaminyltransferase.

†To whom correspondence may be addressed. E-mail: r.jennemann@dkfz.de or h.-j.groene@dkfz-heidelberg.de.

‖Glycosphingolipids are abbreviated according to the recommendations of the International Union of Pure and Applied Chemistry–International Union of Biochemistry Joint Commission on Biochemical Nomenclature of Glycolipids (1).

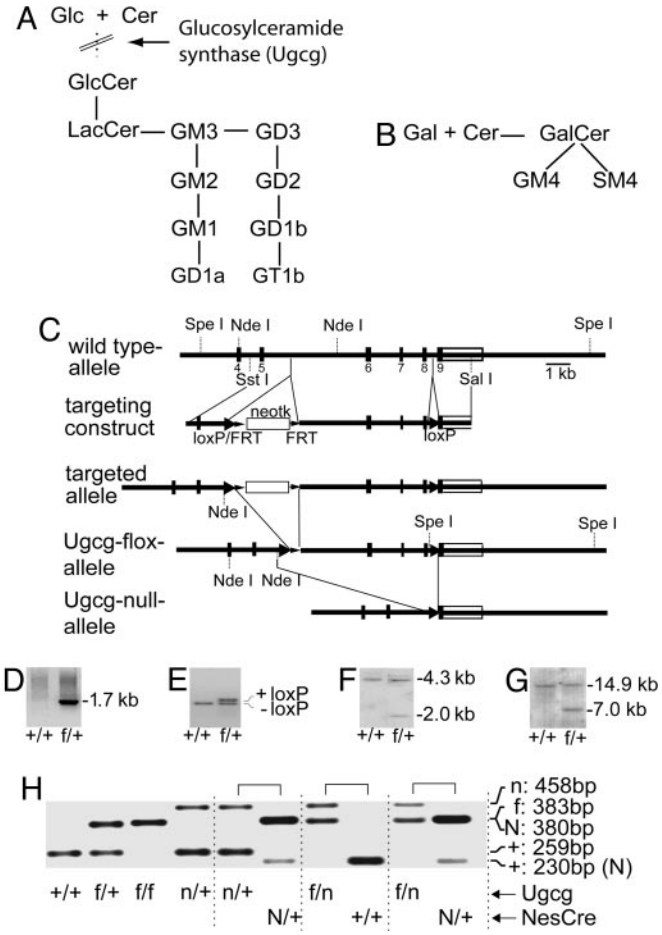

Fig. 1. Major GSL pathways and cloning strategy for *Ugcg* gene deletion and genotyping. (*A*) Glucosylceramide (GlcCer)-based GSLs, including gangliosides, expected to be absent after disruption of the *Ugcg* gene in the brain. (*B*) Galactosylceramide-based GSLs will not be deficient. (*C*) Cloning strategy for the disruption of the *Ugcg* gene. (*D–G*) Genotyping of mutant ES cells and mice by Southern analysis and PCR. (*D*) 5′ targeted stem cells as shown by PCR were indicated by the appearance of a 1.7-kb fragment. (*E*) The integration of the 3′ single loxP site was also shown by PCR. (*F* and *G*) The correctness of *Ugcg*$^{flox/+}$ mice was verified by Southern blot resulting in 5′ hybridization to a 2.0-kb Nde I fragment and in a 3′ Southern blot to a 7.0-kb Spe I fragment of the ''floxed'' allele, respectively. (*H*) Neural cell-specific *Ugcg*$^{null/flox//NesCre}$ mice were characterized by PCR. n, Null; f, flox; N, nestin–Cre; +, wild type.

mRNA Analysis. Total mRNA was analyzed as described in *Supporting Methods*.

Light Microscopy, Immunohistochemistry, and Electron Microscopy. Mice were perfused at P10/P15, or organs were fixed by immersion at E11.5/E15.5/P0/P5 with phosphate-buffered 4% formaldehyde. Tissue was embedded in paraffin wax. Three-micrometer sections were stained by hematoxylin/eosin (H&E) and Nissl stain (Chroma, Köngen, Germany). Immunohistochemistry was performed as described in ref. 17. For type of antibodies, see *Supporting Methods*.

TUNEL was performed according to the *In Situ* Cell Death Detection kit's instructions (Roche, Mannheim, Germany). Apoptotic cells were counted in 20 high-power fields (HPF, ×400) of brain cortex and cerebellum and were given as cells per HPF. For electron microscopy, freshly dissected femoral nerves and brain were fixed in 2.5% glutaraldehyde and processed as described in *Supporting Methods*.

***In Vitro* Culture of Neurons.** Cells from *Ugcg*$^{null/flox//NesCre}$ embryos and *Ugcg*$^{null/flox//+/+}$ controls were isolated from hippocampus at E15.5 and cultivated for 6 days (for further details, see *Supporting Methods*). The neurite and axonal lengths of single cells were determined as in ref. 18. Axonal and neuronal branching points were counted.

Physiological Tests. A righting test was performed according to Ronca and Alberts (19). A test for the ability to maintain position on a rotating rod (Rotorod, SmartRod, AccuScan Instruments, Columbus, OH) was performed at a permanent speed of 2 cm/s and the latency to fall was recorded three times per animal.

Results

***Ugcg*$^{null/flox//NesCre}$ Mice Lack GlcCer-Based GSLs in the Brain.** To verify the disruption of the *Ugcg* gene, brain tissue and spinal cord were analyzed to confirm the absence of these components from E15.5. All GlcCer-based gangliosides were virtually absent from brains of Ugcg-deficient mice (Fig. 2 *A* and *C*) and were already deleted at E15.5 (Fig. 7*A*, which is published as supporting information of the PNAS web site). Traces of GSLs (3–4% of the content in control mice) were detected, possibly because of failed deletion of the floxed *Ugcg* allele in cells with low Cre recombinase activity. Gangliosides were shown to be distributed throughout different brain regions at P10 (Fig. 7*B*).

In the neutral GSL brain fraction of littermates, no significant differences could be observed (Fig. 2*B*). The total content of hexosylceramide (HexCer) in brain of *Ugcg*$^{null/flox//NesCre}$ mice was similar compared with control littermates (Fig. 2*D*). HexCer was shown to be GalCer only, by TLC (Fig. 8, which is published as supporting information on the PNAS web site). Neutral, as well as acidic GSL fractions isolated from liver and kidney of the *Ugcg*$^{null/flox//NesCre}$ and control littermates displayed qualitatively comparable lipid compositions (Fig. 2 *A* and *B*).

Ceramide concentration in brains of *Ugcg*$^{null/flox//NesCre}$ mice decreased from 1.7-fold at P0 to similar or lower levels at P15 as compared with controls (Fig. 2*E*). In contrast, the sphingomyelin content increased consistently in Ugcg-deficient mice after birth (Fig. 2*F*). The molar increase in sphingomyelin was approximately equivalent to the loss of gangliosides (compare Fig. 2 *C* and *F*). No significant differences in the phosphatidylcholine levels could be determined between *Ugcg*$^{null/flox//NesCre}$ mice and controls (data not shown).

Ugcg mRNA Expression in Brain of *Ugcg*$^{null/flox//NesCre}$ Mice Is Significantly Decreased. The disruption of the *Ugcg* gene, as shown by the absence of the GlcCer-based gangliosides in the brain, was confirmed by quantitative real-time RT-PCR. Ugcg-mRNA expression in brain of *Ugcg*$^{null/flox//NesCre}$ mice was almost null compared with *Ugcg*$^{null/flox//+/+}$ and *Ugcg*$^{flox/+//+/+}$ controls ($P < 0.001$ and $P < 0.0001$, respectively). In contrast, the mRNA levels in liver, kidney, and heart of *Ugcg*$^{null/flox//NesCre}$ mice did not show significant differences compared with the *Ugcg*$^{null/flox//+/+}$ control group (Fig. 2 *G–J*). These results indicated deletion of the floxed *Ugcg* allele specifically in neural cell-derived tissue by the nestin gene-promoted Cre recombinase.

***Ugcg*$^{null/flox//NesCre}$ Mice Show Severe Functional Abnormalities.** *Ugcg*$^{null/flox//NesCre}$ embryos developed quite normally (Fig. 9, which is published as supporting information on the PNAS web site) and newborn animals could not be distinguished from their littermates. After birth, Ugcg-deficient mice gained less weight than their control littermates (Fig. 3*A*). Starting at P5–7, *Ugcg*$^{null/flox//NesCre}$ animals developed severe ataxia, indicated by a shuffling gait, as well as strong equilibrium disturbances. The animals frequently dropped sideways without external contact. After P10, the neural defects worsened dramatically, and all *Ugcg*$^{null/flox//NesCre}$ mice died within 24 days (median of 18 days, Fig. 3*B*). Elimination of

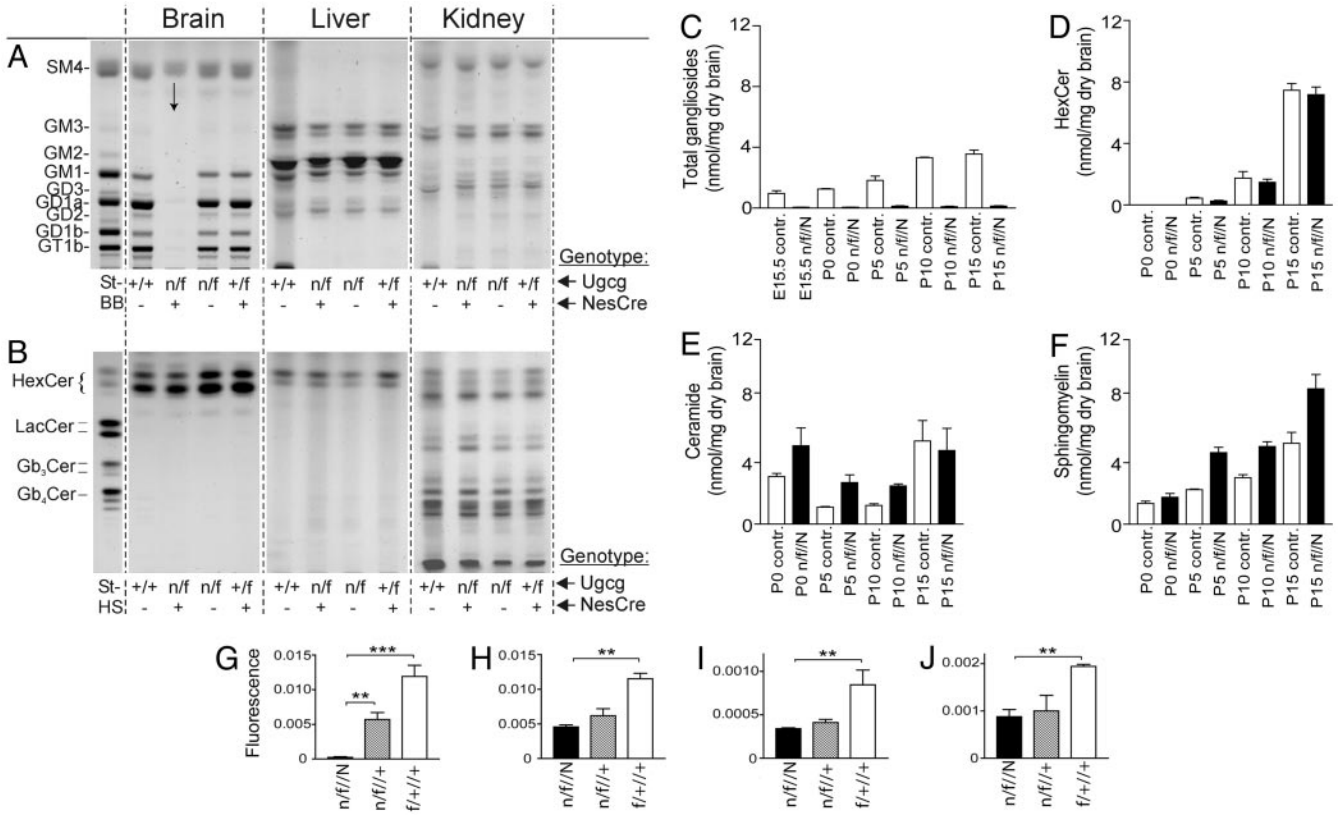

Fig. 2. Sphingolipid and Ugcg mRNA analysis. (*A* and *B*) Acidic (*A*) and neutral (*B*) GSLs separated by TLC and stained as described in ref. 15. Deletion of gangliosides was found in *Ugcg*$^{null/flox//NesCre}$ mice only (*A* arrow). GSL amounts corresponded to 0.5 mg of dry brain and 3.0 mg of dry liver/kidney tissue. St, standards from BB, bovine brain; HS, human spleen. (*C–F*) Quantitation of sphingolipids by densitometry (*C*) and electrospray ionization/tandem mass spectrometry (*D–F*). (*G–J*) mRNA levels in mutant animals: brain (*G*), liver (*H*), kidney (*I*), and heart (*J*). Results are presented as mean ± SEM. **, $P < 0.001$; ***, $P < 0.0001$. Amount of Ugcg mRNA of *Ugcg*$^{null/flox//+/+}$ and *Ugcg*$^{null/flox//NesCre}$ mice in *H–J* was ≈50% of *Ugcg*$^{flox/+//+/+}$ animals. Solely mRNA from brain of *Ugcg*$^{null/flox//NesCre}$ mice was almost completely erased (*G*). n, Null; f, flox; N, nestin–Cre; +, wild type.

heterozygous littermates, which might have prevented *Ugcg*$^{null/flox//NesCre}$ mice from accessing the teats of lactating mothers, did not increase the lifespan. The skin of the *Ugcg*$^{null/flox//NesCre}$ mice still contained a fat layer, indicating that mice did not die of malnutrition. In addition, blood levels of triglycerides and urea showed no significant change. Organs (heart, lung, thymus, liver, spleen, and kidney) were normal by light and electron microscopy except for smaller size compared with controls.

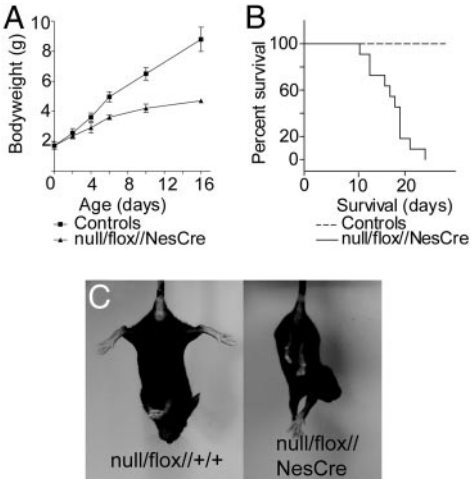

Fig. 3. Body weight, survival, and flight reflex. (*A*) With advancing age, the bodyweight of *Ugcg*$^{null/flox//NesCre}$ mice lagged increasingly behind that of their control littermates. (*B*) Survival rate of *Ugcg*$^{null/flox//NesCre}$ mice. (*C*) When hung by their tails, *Ugcg*$^{null/flox//NesCre}$ mice brought their hind limbs to midline, whereas control animals splayed them widely.

When hung by their tails, affected mice brought their hind limbs to midline, whereas control animals splayed them widely (Fig. 3*C*). A further index of motility disturbance in the *Ugcg*$^{null/flox//NesCre}$ mice was evident by the decreased ability to move back to their limbs after being turned onto their ridge. These animals needed ≈6 s to roll over, far more time than their control littermates, which were able to turn in <0.5 s ($P < 0.0001$). *Ugcg*$^{null/flox//NesCre}$ animals ($n = 4$) failed completely to maintain balance on the top of a rotating rod, whereas control mice ($n = 4$) were able to remain for 1 min, 50 s ± 40 s at a speed of 2 cm/s. The ratio of brain to body weight showed no significant difference between *Ugcg*$^{null/flox//NesCre}$ and control animals.

Homozygous floxed *Ugcg*$^{flox/flox//NesCre}$ mice displayed a phenotype similar to that of *Ugcg*$^{null/flox//NesCre}$ animals.

Phenotypic Structural Analysis. An extensive structural and molecular biology analysis was undertaken to explain the pronounced clinical symptoms. Significant differences in the brains of *Ugcg*$^{null/flox//NesCre}$ mice and control littermates could not be observed by light microscopy at P15 (Fig. 4 *A–D*). By immunohistochemistry, Purkinje cells and hippocampus of control animals expressed the complex ganglioside GD1a, whereas Ugcg-deficient brains stained negative (Fig. 10 *C–F*, which is published as supporting information on the PNAS web site).

Nestin expression was shown in the neural tube at E11.5 (Fig.

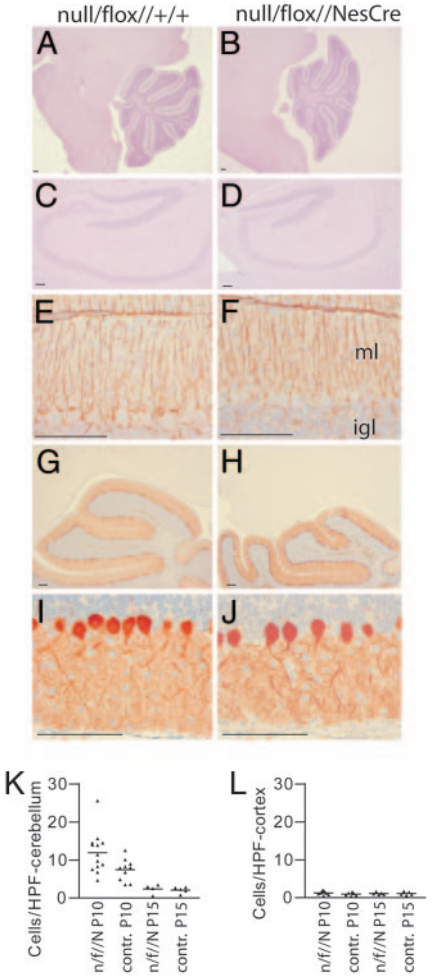

Fig. 4. Brain morphology. (*A–D*) Sagittal view of a *Ugcg*$^{null/flox//+/+}$ (control) (*A* and *C*) and *Ugcg*$^{null/flox//NesCre}$ brain (*B* and *D*) at P15 with similar morphology. (*A–D*) Hematoxylin/eosin staining of cerebellum, brainstem, and part of the cortex (*A* and *B*); hippocampus (*C* and *D*). (*E* and *F*) Glial fibrillary acidic protein immunohistochemistry showed no significant differences between controls (*E*) and the Ugcg-deficient animals (*F*) at P15. igl, internal granular layer; ml, molecular layer of the cerebellum. (*G–J*) Anti-calbindin staining of the Purkinje cell layer. Dendritic tree of Purkinje cells is generally thinner and less complex in *Ugcg*$^{null/flox//NesCre}$ mice (*H* and *J*) as compared with the controls (*G* and *I*). (Scale bars: 100 μm.) (*K* and *L*) Apoptotic cells verified by TUNEL assay, in cerebellum (*K*) and cortex (*L*). Solely in cerebellum of Ugcg-deficient mice (n/f//N), a slight statistical difference was observed at P10.

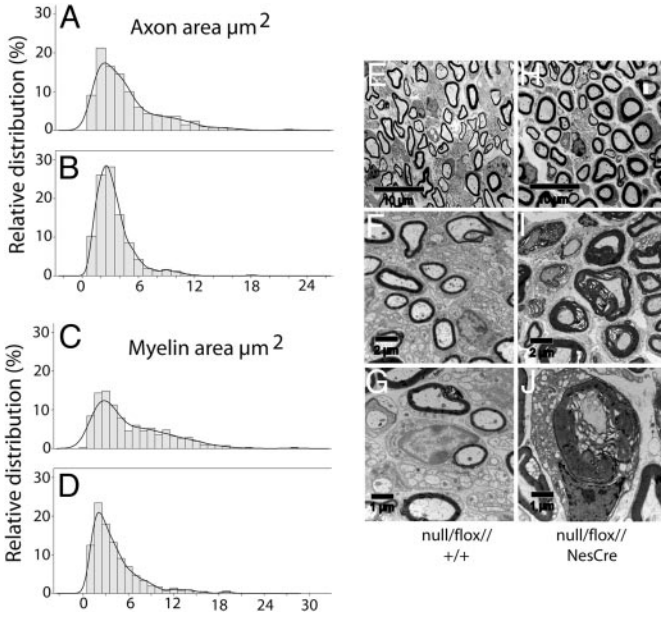

Fig. 5. Electron micrographs of peripheral nerves showed degenerations in axons and myelin. (*A–D*) Relative percentage distribution of areas from femoral nerve axons (n = 419; *A* and *B*) and myelin (*C* and *D*). *Ugcg*$^{null/flox//NesCre}$ mice (*A* and *C*) and controls (*B* and *D*) at P10 to P15. *Ugcg*$^{null/flox//NesCre}$ mice showed an increased number of hypertrophic nerve axons (*A*) with larger myelin areas (*C*) as compared with their control littermates (*B* and *D*), with respective significant differences $P < 0.0001$; Wilcoxon test. Controls (*E–G*) showed thinner myelin sheaths than *Ugcg*$^{null/flox//NesCre}$ mice (*H–J*). Some of the investigated *Ugcg*$^{null/flox//NesCre}$ animals showed pronounced degenerations of nerve axons and myelin sheaths with extensive splitting of the broad myelin sheath (*I* and *J*).

10*G*), in neuroepithelial cells at E15.5 (Fig. 10*I*), and in the femoral nerve (Fig. 10 *K* and *L*). Glial fibrillary acidic protein immunohistochemistry did not reflect any striking changes in the organization of astrocytes [e.g., within the internal granule cell layer or in the dendritic extension of the Bergmann glia in the molecular layer of the cerebellum (Fig. 4 *E* and *F*)]. By calbindin staining, the dendritic tree of the Purkinje cells, however, showed a decreased height and arborization in *Ugcg*$^{null/flox//NesCre}$ cerebella (height: *Ugcg*$^{null/flox//NesCre}$, 108 ± 12.8 vs. control, 138 ± 10.6 μm, n = 4 each; branches per high-power field: *Ugcg*$^{null/flox//NesCre}$, 56.9 ± 2.1 vs. control, 66.5 ± 2.4; n = 3 each, 30 cells per animal; Fig. 4 *G–J*).

By immunohistochemistry, myelin-associated glycoprotein, neuron-specific nuclear protein, and amyloid-β precursor protein displayed no different expression of the proteins in brains of *Ugcg*$^{null/flox//NesCre}$ animals as compared with controls (Fig. 10 and data not shown).

The number of apoptotic cells in the cerebella of *Ugcg*$^{null/flox//NesCre}$ animals and control mice overlapped at P10; also, differences were not apparent between the two groups at P15 (Fig. 4*K*). The mean number of apoptotic cells in the cortex was considerably lower than in the cerebellum, again with no differences between the *Ugcg*-deficient and control mice (Fig. 4*L*).

Concomitantly with the results obtained from TUNEL, proliferating cells as detected by Ki67 antibody were seldom seen in both groups (data not shown).

By electron microscopy, synapses of Purkinje cells appeared similar in structure between Ugcg-deficient and control mice.

Peripheral Nerve Axons and Myelin Sheaths of *Ugcg*$^{null/flox//NesCre}$ Mice Are Enlarged. In Ugcg-deficient mice, ultrastructural investigations of the femoral nerve revealed an increased surface area for both axon (Fig. 5 *A* vs. *B*) and myelin (Fig. 5 *C* vs. *D* and *H–J* vs. *E–G*); Wilcoxon test, $P < 0.0001$ for both parameters. In some Ugcg-deficient animals, a pronounced splitting of the myelin sheaths could be seen [Fig. 5 *I* and *J* (*Ugcg*$^{null/flox//NesCre}$) vs. *F* and *G* (controls)].

***Ugcg*$^{null/flox//NesCre}$-Derived Neural Cells Display Restricted Neurite Outgrowth.** In view of the alterations seen in neurons, specifically Purkinje cells of *Ugcg*$^{null/flox//NesCre}$ mice, the development of hippocampal neurons was further examined in culture. Gangliosides were detected in hippocampus of E15.5 control animals in moderate amounts (Fig. 7*C*).

The neurite length and number of branching points were clearly diminished in the primary cultures of neurons of E15.5 embryos from *Ugcg*$^{null/flox//NesCre}$ mice (Fig. 6 *A* and *B* vs. *C* and *D*). The total neurite length was significantly reduced in neurons of Ugcg-deficient animals (≈1/3 of that from control animals; $P < 0.001$, Fig.

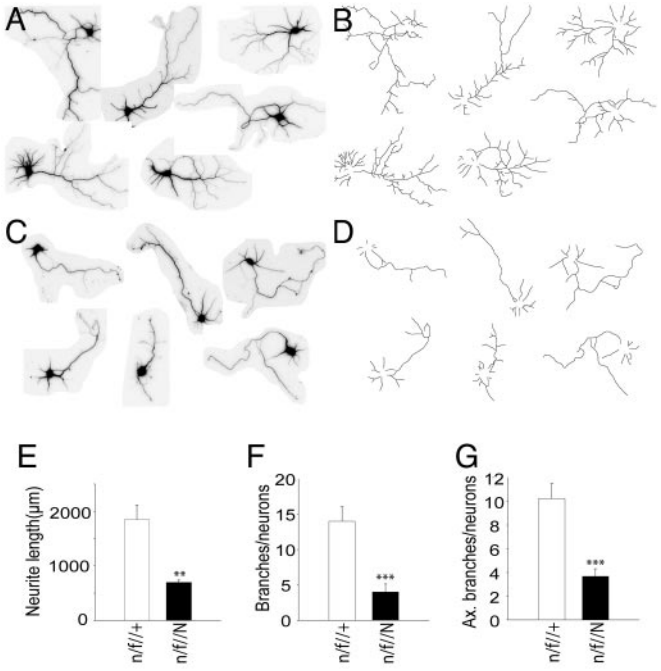

Fig. 6. Primary cultured neuronal cells have restricted potential to form dendritic extensions. Neurite length and axonal length from 30–40 representative neuronal cells isolated from hippocampus of *Ugcg*$^{null/flox//NesCre}$ embryos and controls at E15.5 ($n = 3$ for each) were determined and calculated with PHOTOSHOP (Adobe Systems, San Jose, CA) at culture-day 6. Numbers of dendritic and axonal branches were counted (means ± SEM). Shown are photographs (*A* and *C*) and corresponding drawings (*B* and *D*) of primary neuronal cells for calculation of dendrite length (*B* and *D*) from *Ugcg*$^{null/flox//+/+}$ (*A* and *B*) and *Ugcg*$^{null/flox//NesCre}$ (*C* and *D*) embryos. (*E*) The neurite length of cultured neuronal cells from Ugcg-deficient embryos was significantly diminished to ≈1/3 of controls ($P < 0.001$). Significantly decreased numbers of neuronal branching points in the Ugcg-deficient cells (*F*) correlated well with the reduced axonal branches (*G*) ($P < 0.000002$ and $P < 0.00005$, respectively). n, Null; f, flox; N, nestin–Cre; +, wild type.

6*E*). The axonal length was not changed in *Ugcg*$^{null/flox//NesCre}$ animals as compared with controls. Furthermore, the number of neuronal and axonal branches was significantly lower ($P < 2 \times 10^{-6}$ and $P < 5 \times 10^{-5}$, Fig. 6 *F* and *G*). As compared with *Ugcg*$^{null/flox//+/+}$ controls, neurons from *Ugcg*$^{null/flox//NesCre}$ mice showed signs of early and pronounced axonal pruning (Fig. 11, which is published as supporting information on the PNAS web site).

mRNA Expression. Transcriptional profiling was performed to obtain information on hitherto unknown cellular processes, which might be influenced by the disruption of the *Ugcg* gene.

Analysis showed 310 of 8,117 genes (≈4%) differentially regulated; the majority of these genes were down-regulated (Fig.12, which is published as supporting information on the PNAS web site).

When analyzed by gene set enrichment analysis with curated lists of functional pathways, eight pathways were found to be significantly altered, e.g., MAP-kinase-, WNT-, and CXCR4-signaling-pathways. G protein-coupled receptor signaling in general was down-regulated at different key levels (Table 1, which is published as supporting information on the PNAS web site).

Discussion

GSLs, in particular the GlcCer-derived gangliosides, occur in the brain at a much higher concentration (10) than in other organs of mesodermal or endodermal origin (20). They may, therefore, play an important functional role in the nervous system.

The majority of all mammalian GSLs are derived from precursor GlcCer. Therefore, the gene encoding the enzyme that catalyzes the initial step of GSL biosynthesis, *Ugcg*, is a key regulator of GSL synthesis. The systemic disruption of this gene in mice is lethal during early embryogenesis (9). To gain knowledge about brain-specific functions of GSLs, a nestin gene-driven neural cell type-restricted disruption of the *Ugcg* gene in mice was established. Nestin, an intermediate filament protein of neuroepithelial stem cells, is expressed in neural stem cells and peripheral nerves. Our results are in concordance with earlier reports that could show nestin expression at E9.5 to E12 in neural tissue (21, 22). The early expression of nestin-*cre* is fundamental for the specific deletion of the *Ugcg* gene during brain ontogenesis.

The cell-specific disruption of the *Ugcg* gene in neural progenitor cells, as described here, was associated with the absence of virtually all GlcCer-based GSL in embryonic and postnatal brain.

In *Ugcg*$^{null/flox//NesCre}$ mice, galactosylceramide-derived GSLs did not compensate for GlcCer-based GSLs. In contrast, in mouse mutants with a total inactivation of ceramide galactosyltransferase, a marked increase in GlcCer concentration was observed (23).

A total disruption of the *N*-acetylgalactosaminyltransferase (*GalNAcT*) gene in mice resulted in a complete loss of the complex gangliosides and an increase in both precursors, GM3 and GD3 (24). In these GalNAcT$^{-/-}$ mice, embryonic development or lifespan was not changed, as compared with controls. However, with increasing age, mild gait disturbances and degenerations in sciatic nerves have been described.

Mice expressing only ganglioside GM3, generated with simultaneously disrupted *GalNAcT* and *sialyltransferase II* genes, showed a stronger phenotype displaying hypertrophic nerve fibers, peripheral nerve degeneration, muscaric and sensoric dysfunction, and gait disturbance with aging. The survival rate in mice expressing only GM3 ranged between 10 and 60 weeks (25, 26). Apparently with decreasing complexity of GSL, neurologic disease manifests itself earlier and more severely.

Ugcg$^{null/flox//NesCre}$ embryos were indistinguishable from the null mutants as judged macroscopically and by light microscopy. Nevertheless, the absence of GSL could already be demonstrated at E15.5. Newborn animals could not be distinguished from their heterozygous littermates. This observation indicates that GSLs may not be essential during embryonic ontogenesis of the nervous system. Already starting from P5 to P7, first signs of ataxia could be observed in *Ugcg*$^{null/flox//NesCre}$ mice. After P10, the neural defects worsened dramatically and were associated with relevant abnormalities in neural cell differentiation (e.g., Purkinje cells). All mice died within 24 days.

All through embryogenesis, GSL concentrations in brain are indeed very low (only 1/4 of postnatal concentrations at P10/15; Figs. 2*C* and 7) and increase appreciably only after birth, simultaneously with the postnatal differentiation of the brain. Symptoms apparently show up only during this time and not before birth.

In support of this perception, it has been reported that a disruption of synthesis of complex gangliosides in axons of mice leads to an interruption of the interaction of gangliosides with complementary lectin-binding partners, e.g., myelin-associated glycoprotein, months after birth (27). In this study, the morphologic sequelae were axon degeneration. Functional neurologic tests, such as the hind limb reflex, demonstrated defects in motor coordination. The authors of ref. 27 also interpreted their data to mean that GSLs were important for the axon-myelin architecture in brain maturation but less essential during embryogenesis.

Symptoms in mice with Ugcg deficiency occur shortly after birth in a most severe form obviously due to the complete deficiency of gangliosides and neutral GSL.

Comparable concentrations of serum triglycerides and urea between Ugcg-deficient and control animals demonstrated that the Ugcg-deficient mice were not in a catabolic state and did not die of

malnutrition. The direct cause of death could not be established, but death was probably initiated by the severe neurologic deficits.

In GalNAcT$^{-/-}$ mice, gangliosides GM3 and/or GD3 were presumably able to substitute for the function of the complex gangliosides to a certain degree, whereas animals lacking all GlcCer-based GSLs in the brain could not compensatorily use other glycoconjugates, developed severe neurologic deficits, and died postnatally at a very early stage. Observations, comparable to GalNAcT$^{-/-}$, have been described recently in mice with deleted *GalNAc*T/*sialyltransferase 9* genes that were unable to synthesize ganglio-series gangliosides (28). Perhaps as compensation, these mice synthesize lacto-series gangliosides and increased amounts of SM3 in the brain, leading to a higher life expectancy (>5 months), as compared with our Ugcg-deficient animals.

Several reports have suggested that gangliosides could play a trophic role in the nervous system, because exogenously applied gangliosides induced differentiation of neuronal cells in culture with enhanced axonal sprouting and neurite outgrowth (for review, see ref. 29). In the present study, significant although moderate differences in neurite formation were observed between *Ugcg*$^{\text{null/flox//NesCre}}$ and control brains by light microscopy. To unequivocally document a reduction in neuron branching, the growth of neuronal cells of Ugcg-deficient and control mice has been studied in culture. Here, the lack of all brain gangliosides had a strong influence on the outgrowth of dendrites with regard to their length and arborization. Furthermore, neurons from *Ugcg*$^{\text{null/flox//NesCre}}$ mice showed signs of early axonal pruning.

Ugcg$^{\text{null/flox//NesCre}}$ mice, which lack all gangliosides, formed hypertrophic axons and myelin sheaths rather similar to those previously observed for mice expressing only ganglioside GM3 (25) but at a much earlier time.

A destabilization in axon–myelin interaction caused by the absence of GSL, as potential ligands on the axonal membranes, to myelin-associated glycoprotein in the oligodendritic cell myelin membranes (30) might be one reason for the disturbed myelin arrangement with broadened and split sheaths.

In addition, a direct influence on myelin maturation by the absence of GlcCer-based GSL cannot be excluded (31, 32). GalNAcT$^{-/-}$ mice, lacking complex gangliosides and expressing only the precursors GM3/GD3, showed myelination defects in older animals, as well as axonal degenerations (33).

Ugcg uses ceramide as one of its substrates. Deletion of enzyme activity could lead to a rise in ceramide concentration and to apoptosis (34, 35). Animals at P15 did not express higher ceramide concentrations and more apoptotic cells in the brain than their controls and, therefore, ceramide was not likely to have contributed to brain dysfunction of the *Ugcg*$^{\text{null/flox//NesCre}}$ mice. Ceramide was apparently converted into sphingomyelin, which proportionally increased postnatally, thus, possibly substituting for some function normally associated with the gangliosides.

Deficiency or lack of the majority of GSLs in the nervous system was associated with a significant down-regulation of numerous mRNA profiles in brain. Although these changes in steady-state mRNAs could well be a secondary event, several respective genes have been implicated in neuron development and function. In yeast, lack of GSLs has been reported to influence mRNAs of genes involved in numerous metabolic pathways and nuclear processes (36). By gene set enrichment analysis, it could be seen that the mRNA of proteins involved in signaling for G protein-coupled receptors and, specifically for the CXCL12 (SDF1)-CXCR4 chemokine receptor pair, was tuned down. Both CXCL12 and its receptor serve essential functions in brain development (37). Our data point to an influence of GSLs not only on membrane composition and interactions with membrane proteins but also on expression of genes essential for brain development and homeostasis. How these effects of GSLs are exerted at the molecular level remains unresolved at this time point.

Recently, it was convincingly demonstrated that humans carrying a homozygous mutation in the *GM3-synthase* gene suffered from an infantile-onset symptomatic epilepsy syndrome, associated with developmental stagnation and blindness (38). Therefore, mutations of GSL-synthesis enzymes leading to absence of specific structures, and not only mutations of GSL-degrading enzymes associated with accumulation of those GSL, can cause relevant clinical symptoms.

The neuronal-specific deficiency of GlcCer synthesis in mice indicates that GlcCer-derived GSLs may not serve functions essential for early brain development. They would, however, be functionally required for neuron differentiation and brain maturation.

We thank R. Fässler for helpful instructions for the stem cell cultivation; F. Vanderhoeven and U. Klotz for blastocyst injections; G. Schütz for provision of the Cre- and FLP-mice; R. Kuner for help in physiological tests; M. Schulze, T. Manoli, and L. Li for evaluation of gene array data; J. Trotter and P. Nelson for helpful discussion; and S. Kaden, U. Rothermel, C. Schmidt, and G. Schmidt for superb technical assistance. This work was supported by Deutsche Forschungsgemeinschaft Grants SFB 405: B10 and Graduiertenkolleg 886 to H.-J.G.

1. IUPAC–IUB Joint Commission on Biochemical Nomenclature of Glycolipids (1999) *J. Mol. Biol.* **286**, 963–970.
2. Hakomori, S. (1990) *J. Biol. Chem.* **265,** 18713–18716.
3. Nagai, Y. & Tsuji, S. (1994) *Prog. Brain Res.* **101,** 119–126.
4. Hidari, K., Ichikawa, S., Fujita, T., Sakiyama, H. & Hirabayashi, Y. (1996) *J. Biol. Chem.* **271,** 14636–14641.
5. Varki, A. (1993) *Glycobiology* **3,** 97–130.
6. Sprong, H., Degroote, S., Claessens, T., van Drunen, J., Oorschot, V., Westerink, B. H., Hirabayashi, Y., Klumperman, J., van der Sluijs, P. & van Meer, G. (2001) *J. Cell Biol.* **155,** 369–380.
7. Degroote, S., Wolthoorn, J. & van Meer, G. (2004) *Semin. Cell. Dev. Biol.* **15,** 375–387.
8. Ichikawa, S., Ozawa, K. & Hirabayashi, Y. (1998) *Biochem. Biophys. Res. Commun.* **253,** 707–711.
9. Yamashita, T., Wada, R., Sasaki, T., Deng, C., Bierfreund, U., Sandhoff, K. & Proia, R. L. (1999) *Proc. Natl. Acad. Sci. USA* **96,** 9142–9147.
10. Yu, R. K. & Saito, M. (1989) in *Neurobiology of Glycoconjugates*, eds. Margolis, R. U. & Margolis, R. K. (Plenum, New York), pp. 1–42.
11. Tronche, F., Kellendonk, C., Kretz, O., Gass, P., Anlag, K., Orban, P. C., Bock, R., Klein, R. & Schutz, G. (1999) *Nat. Genet.* **23,** 99–103.
12. Li, E., Bestor, T. H. & Jaenisch, R. (1992) *Cell* **69,** 915–926.
13. Schwenk, F., Baron, U. & Rajewsky, K. (1995) *Nucleic Acids Res.* **23,** 5080–5081.
14. Rodriguez, C. I., Buchholz, F., Galloway, J., Sequerra, R., Kasper, J., Ayala, R., Stewart, A. F. & Dymecki, S. M. (2000) *Nat. Genet.* **25,** 139–140.
15. Jennemann, R., Rodden, A., Bauer, B. L., Mennel, H. D. & Wiegandt, H. (1990) *Cancer Res.* **50,** 7444–7449.
16. Sandhoff, R., Hepbildikler, S. T., Jennemann, R., Geyer, R., Gieselmann, V., Proia, R. L., Wiegandt, H. & Gröne, H. J. (2002) *J. Biol. Chem.* **277,** 20386–20398.
17. Gröne, H. J., Cohen, C. D., Gröne, E., Schmidt, C., Kretzler, M., Schlondorff, D. & Nelson, P. J. (2002) *J. Am. Soc. Nephrol.* **13,** 957–967.
18. Rico, B., Beggs, H. E., Schahin-Reed, D., Kimes, N., Schmidt, A. & Reichardt, L. F. (2004) *Nat. Neurosci.* **7,** 1059–1069.
19. Ronca, A. E. & Alberts, J. R. (2000) *J. Appl. Physiol.* **89,** 2318–2324.
20. Nakamura, K., Hashimoto, Y., Yamakawa, T. & Suzuki, A. (1988) *J. Biochem. (Tokyo)* **103,** 201–208.
21. Zimmerman, L., Parr, B., Lendahl, U., Cunningham, M., McKay, R., Gavin, B., Mann, J., Vassileva, G. & McMahon, A. (1994) *Neuron* **12,** 11–24.
22. Mantamadiotis, T., Lemberger, T., Bleckmann, S. C., Kern, H., Kretz, O., Martin Villalba, A., Tronche, F., Kellendonk, C., Gau, D., Kapfhammer, J., *et al.* (2002) *Nat. Genet.* **31,** 47–54.
23. Bosio, A., Binczek, E. & Stoffel, W. (1996) *Proc. Natl. Acad. Sci. USA* **93,** 13280–13285.
24. Takamiya, K., Yamamoto, A., Furukawa, K., Yamashiro, S., Shin, M., Okada, M., Fukumoto, S., Haraguchi, M., Takeda, N., Fujimura, K., *et al.* (1996) *Proc. Natl. Acad. Sci. USA* **93,** 10662–10667.
25. Inoue, M., Fujii, Y., Furukawa, K., Okada, M., Okumura, K., Hayakawa, T. & Sugiura, Y. (2002) *J. Biol. Chem.* **277,** 29881–29888.
26. Kawai, H., Allende, M. L., Wada, R., Kono, M., Sango, K., Deng, C., Miyakawa, T., Crawley, J. N., Werth, N., Bierfreund, U., *et al.* (2001) *J. Biol. Chem.* **276,** 6885–6888.
27. Pan, B., Fromholt, S. E., Hess, E. J., Crawford, T. O., Griffin, J. W., Sheikh, K. A. & Schnaar, R. L. (2005) *Exp. Neurol.* **195,** 208–217.
28. Yamashita, T., Wu, Y. P., Sandhoff, R., Werth, N., Mizukami, H., Ellis, J. M., Dupree, J. L., Geyer, R., Sandhoff, K. & Proia, R. L. (2005) *Proc. Natl. Acad. Sci. USA* **102,** 2725–2730.
29. Ledeen, R. W., Wu, G., Lu, Z. H., Kozireski-Chuback, D. & Fang, Y. (1998) *Ann. N.Y. Acad. Sci.* **845,** 161–175.
30. Vyas, A. A., Patel, H. V., Fromholt, S. E., Heffer-Lauc, M., Vyas, K. A., Dang, J., Schachner, M. & Schnaar, R. L. (2002) *Proc. Natl. Acad. Sci. USA* **99,** 8412–8417.
31. Ogawa-Goto, K. & Abe, T. (1998) *Neurochem. Res.* **23,** 305–310.
32. Lobsiger, C. S., Smith, P. M., Buchstaller, J., Schweitzer, B., Franklin, R. J., Suter, U. & Taylor, V. (2001) *Glia* **36,** 31–47.
33. Vyas, A. A. & Schnaar, R. L. (2001) *Biochimie* **83,** 677–682.
34. Hannun, Y. A. & Obeid, L. M. (2002) *J. Biol. Chem.* **277,** 25847–25850.
35. van Blitterswijk, W. J., van der Luit, A. H., Veldman, R. J., Verheij, M. & Borst, J. (2003) *Biochem. J.* **369,** 199–211.
36. Cowart, L. A., Okamoto, Y., Pinto, F. R., Gandy, J. L., Almeida, J. S. & Hannun, Y. A. (2003) *J. Biol. Chem.* **278,** 30328–30338.
37. Zou, Y. R., Kottmann, A. H., Kuroda, M., Taniuchi, I. & Littman, D. R. (1998) *Nature* **393,** 595–599.
38. Simpson, M. A., Cross, H., Proukakis, C., Priestman, D. A., Neville, D. C., Reinkensmeier, G., Wang, H., Wiznitzer, M., Gurtz, K., Verganelaki, A., *et al.* (2004) *Nat. Genet.* **36,** 1225–1229.